ADVANCED FUNCTIONAL MATERIALS
www.afm-journal.de

Injectable Plasma-Treated Alginate Hydrogel for Oxidative Stress Delivery to Induce Immunogenic Cell Death in Osteosarcoma

*Milica Živanić, Albert Espona-Noguera, Hanne Verswyvel, Evelien Smits, Annemie Bogaerts, Abraham Lin, and Cristina Canal**

Cold atmospheric plasma (CAP) is a source of cell-damaging oxidant molecules that may be used as low-cost cancer treatment with minimal side effects. Liquids treated with cold plasma and enriched with oxidants are a modality for non-invasive treatment of internal tumors with cold plasma via injection. However, liquids are easily diluted with body fluids which impedes high and localized delivery of oxidants to the target. As an alternative, plasma-treated hydrogels (PTH) emerge as vehicles for the precise delivery of oxidants. This study reports an optimal protocol for the preparation of injectable alginate PTH that ensures the preservation of plasma-generated oxidants. The generation, storage, and release of oxidants from the PTH are assessed. The efficacy of the alginate PTH in cancer treatment is demonstrated in the context of cancer cell cytotoxicity and immunogenicity–release of danger signals and phagocytosis by immature dendritic cells, up to now unexplored for PTH. These are shown in osteosarcoma, a hard-to-treat cancer. The study aims to consolidate PTH as a novel cold plasma treatment modality for non-invasive or postoperative tumor treatment. The results offer a rationale for further exploration of alginate-based PTHs as a versatile platform in biomedical engineering.

1. Introduction

Cold atmospheric plasma (CAP) or non-thermal plasma (NTP), from now on referred to as plasma, is a weakly ionized gas that in recent years gained interest as low-cost cancer therapy with minimal side effects.[1] For biomedical applications, plasma is normally generated using dielectric barrier discharge (DBD) devices or atmospheric pressure plasma jets (APPJ), for example, the kINPen device.[1–3] There are different physical (ie. electrical fields) and chemical (ie. reactive species) components of plasmas that may exert a biological effect.[4] In practical terms, plasma represents an exogenous source of reactive oxygen and nitrogen species (RONS), generated following interaction with ambient air, that play an important role in cell physiology and pathology.[5–7] Plasma also interacts with surrounding molecules from the air, liquid, or the (biological) target[8] that results in a complex cocktail of RONS[9,10] comprising highly reactive short-lived species such as ·O, ·OH, and ·NO and more stable, long-lived species, e.g., H_2O_2 and NO_2^-. In high concentrations, RONS can irreversibly alter biomolecules and lead to cell death. Upon exposure to plasma (exogenous addition of RONS), and due to their altered characteristics, malignant cells are more likely than non-malignant cells to reach the cytotoxic threshold and die.[11,12] In addition to this selective cytotoxic effect, plasma treatment could also promote anti-tumor immune responses through different mechanisms.[13] Such responses are important for systemic and long-lasting therapeutic effects that makes plasma a promising adjuvant treatment.

M. Živanić, A. Espona-Noguera, C. Canal
Biomaterials, Biomechanics and Tissue Engineering Group
Department of Materials Science and Engineering
Escola d'Enginyeria Barcelona Est (EEBE) and Research Centre for Biomedical Engineering (CREB)
Universitat Politècnica de Catalunya (UPC)
c/Eduard Maristany 14, Barcelona 08019, Spain
E-mail: cristina.canal@upc.edu

The ORCID identification number(s) for the author(s) of this article can be found under https://doi.org/10.1002/adfm.202312005

DOI: 10.1002/adfm.202312005

M. Živanić, A. Espona-Noguera, C. Canal
Biomaterials and Tissue Engineering
Institut de Recerca Sant Joan de Déu
39-57, Esplugues de Llobregat, Santa Rosa 08950, Spain

M. Živanić, H. Verswyvel, A. Bogaerts, A. Lin
Plasma Lab for Applications in Sustainability and Medicine-Antwerp (PLASMANT)
Department of Chemistry
University of Antwerp
Universiteitsplein 1, Wilrijk, Antwerp 2610, Belgium

H. Verswyvel, E. Smits, A. Lin
Center for Oncological Research (CORE)
Integrated Personalized & Precision Oncology Network (IPPON)
University of Antwerp
Universiteitsplein 1, Wilrijk, Antwerp 2610, Belgium

There are two common ways in which plasma-generated RONS can be delivered to a target: direct delivery with a plasma device or indirect delivery through a plasma-treated liquid (PTL). PTL is a liquid (e.g., Phosphate-buffered saline or Ringer's saline) that was exposed to a plasma device, resulting in its enrichment with long-lived RONS.[9,14] Direct treatment is limited by the plasma penetration depth, as revealed by different surrogate tissue models.[8,15] Compared to direct treatment, PTL administration (injection) does not require direct access to the tumor bed. This makes PTLs especially attractive for the (repeated) treatment of internal tumors. However, liquids are quickly mixed and diluted with the body fluids. Thus, PTLs offer poor control over the delivery of RONS to the target.[13,16] In contrast to direct treatment where a variety of RONS reach the target, PTLs only contain more stable long-lived species (mainly H_2O_2, NO_2^-, NO_3^-) while short-lived RONS are lost due to their quick reaction time. In this context, there is an ongoing debate on whether the chemistry of PTLs can be reduced to peroxide (H_2O_2) chemistry. In other words, if the biological effect of a PTL can be reproduced when the liquid is artificially supplemented with H_2O_2 and NO_2^- solution. This particularly concerns chemically simple liquids, e.g., water. Intuitively, the greater the chemical complexity of the liquid, the more likely it is that its components interact with plasma species for more variable plasma chemistry.[17] For instance, biological effects beyond H_2O_2-induced cell cytotoxicity were more evident for a PTL containing the organic compound lactate.[18]

To address the challenges of PTLs and enable not only minimally-invasive but also precise treatment of internal tumors with plasma, in 2019, our group proposed plasma-treated hydrogels (PTHs), as a novel, third plasma treatment modality.[13,19] To prepare a PTH, a liquid that contains polymers is first treated with plasma to enrich it with RONS. Then, this polymeric solution is cross-linked into a hydrogel, so that RONS remain entrapped within the gel and can be released by simple diffusion once the PTH comes in contact with the biological fluid or target. The crosslinking strategy can be chosen to allow for an injectable hydrogel and its non-surgical administration.[20] Briefly, a hydrogel is a 3D network of hydrophilic polymers and water that has a porous structure and viscoelastic behavior (properties of elastic solid and viscous liquid). As such, hydrogels resemble the extracellular matrix of tissues and are commonly explored for controlled drug delivery, cell encapsulation, and tissue engineering.[21] Thanks to the rich chemistry of polymers and the reactive chemical groups, their presence could contribute to plasma chemistry.[22] For example, treatment of an amino-acid based polymer with plasma favored generation of reactive nitrogen species.[23] In addition, compared to liquids, hydrogels are more viscous and show good retention of material at the site of injection or implantation. Taken together, this implies that PTH could enable high local delivery of RONS to the target.[13] So far, there are two studies that provided evidence of PTH cancer cytotoxicity in vitro[24] and in vivo.[25] In both studies, injectable thermosensitive PTHs that solidify at the body temperature were used. Nevertheless, the investigation on PTHs remains very limited.

Here, we report an injectable, shape-adaptable alginate PTH for cancer treatment. Alginate cross-links quickly in the presence of divalent cations, for example, Ca^{2+}, and is a crucial natural polymer in biomedical engineering thanks to its biocompatibility, biodegradability, and great versatility.[26,27] However, previous attempts to make alginate PTH resulted in the loss of RONS during the crosslinking step and, thus, in the loss of cytotoxic capacity of PTH.[19] In this study, we report an optimized preparation protocol and perform physical, chemical, and biological characterization relevant for the application of PTH as a vehicle for RONS delivery in cancer treatment. While immunogenicity has been previously observed for direct plasma treatment and PTLs,[13,28] there are no such reports for PTHs. Here, for the first time, we investigate if a PTH treatment could promote anti-tumor immune responses, in particular the release of danger signals and phagocytosis by human monocyte-derived dendritic cells, as an initial step in the cancer immunity cycle.[29] For this, we use cell lines of osteosarcoma, a rarely studied cancer with poor prognosis and treatment alternatives for which the immunogenic effect of plasma treatment (direct or indirect) is still unknown. Our research aims to consolidate PTH as a novel plasma treatment modality that could combine RONS-based therapies with hydrogel-based drug delivery and tissue engineering. In relation to this, our study aims to provide an important basis for further improvement and engineering of alginate-based PTHs, as a truly versatile platform in the field of biomedicine.

2. Results

2.1. Injectable Plasma-Treated Hydrogel (PTH): Design and Physical Properties

To obtain an injectable PTH, 0.5% (w/v) aqueous alginate solution was treated with plasma to enrich it with RONS and then cross-linked into the hydrogel (**Figure 1A**). Alginate cross-links rapidly in contact with divalent cations and $CaCl_2$ is a frequently used cross-linker solution. However, such a reaction is immediate and poorly controllable which can result in non-homogenous hydrogel and loss of material. Namely, if $CaCl_2$ is added to alginate solution, only parts with immediate contact will cross-link, while others will remain liquid and be lost. If, on the other hand, alginate is immersed into a $CaCl_2$ solution, loaded molecules (here RONS) will be washed out of the liquid hydrogel phase.[19] To avoid this and ensure the preservation of RONS and injectability of PTH, we used small volume of $CaSO_4$ cross-linker solution (CS) mixed with a salt retardant solution (RS). In this way, the crosslinking reaction was retarded just enough to make PTH injectable but still enable good retention of the material upon its immediate injection in water (Figure 1B; Figure S1, Supporting Information). If extruded continuously into a liquid, the PTH had a filamentous form. On the other hand, if injected into a dry cavity, the PTH showed a form-fitting shape (Figure 1C; Figure S2, Supporting Information). This is interesting from the perspective of applying the PTH to fill the cavity and treat surgical margins upon excision of a tumor mass. Similarly, for the in vitro experiments described here, the conditioned medium was removed from the cells before injecting the PTH to the dry well and on top of the cells. One minute later, a fresh cell culture medium was added. In this way, the PTH (Figure 1A, *bottom right image, white/transparent layer*) covered the entire well for uniform contact with the cells. One minute was already enough for the hydrogel to become solid-like. This can be appreciated in Figure 1D on the example of non-treated hydrogel (NTH), where 1 min after

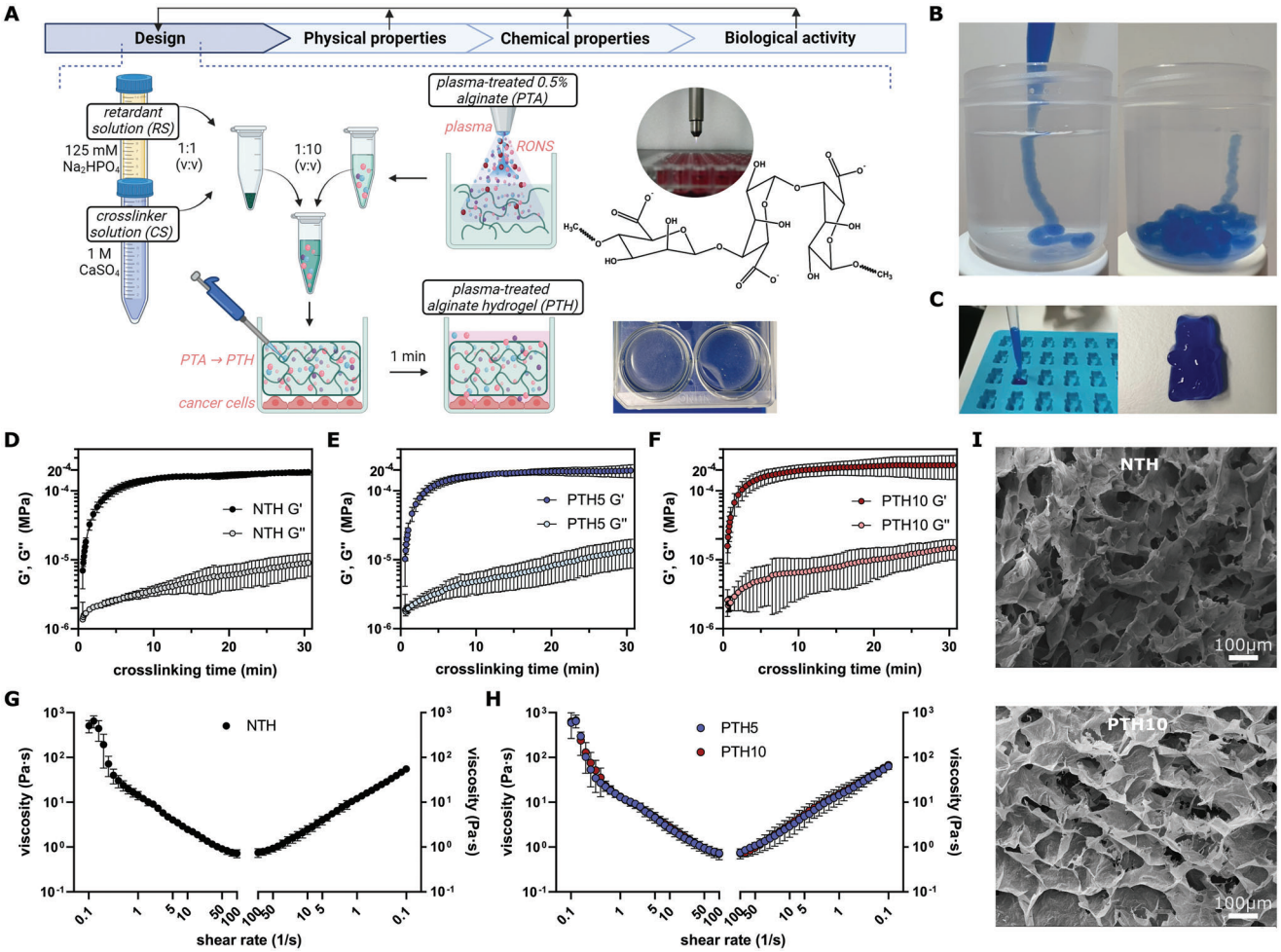

Figure 1. Hydrogel design and physical properties. A) Protocol for preparation of injectable alginate PTH and characterization of workflow. B) Filamentous form of the hydrogel when injected directly into the liquid (here water). C) Shape-fitting form of the hydrogel when injected into a dry cavity. B,C) Hydrogels were loaded with dextran blue for better visualization. D) Hydrogel crosslinking kinetics (injectability window) observed as hydrogel storage (G') and loss (G'') modulus in function of time (with t_0 = initiation of the crosslinking reaction). E,F) Effect of plasma treatment (5 or 10 min) on hydrogel crosslinking kinetics. G) Shear-thinning behavior of fully cross-linked hydrogel (t = 30 min since initiation of the crosslinking reaction) observed as a change in hydrogel viscosity when gradually applying and then releasing shear stress (which mimics injection with a syringe). (H) Effect of plasma treatment (5 or 10 min) on hydrogel shear-thinning behavior. D–H) n = 3, data is presented as mean ± SD. I) Hydrogel microstructure as observed with scanning electron microscopy (SEM). NTH: non-treated hydrogel. PTH5, PTH10: 5 or 10 min plasma-treated hydrogel. Scale bar 100 µm.

the initiation of crosslinking reaction (addition of CS/RS mix to the alginate) the storage modulus (G') was prominently above the loss modulus (G''). However, it took ≈10 min for G' to stabilize (maximal crosslinking), with a mean G' of 187 ± 17 Pa (measured at 1 Hz angular frequency). The crosslinking reaction was not altered when alginate was treated for 5 or 10 min with plasma, with PTH5 and PTH10 having the same crosslinking kinetics and similar maximal G' values (196 ± 42 Pa and 236 ± 90 Pa, respectively) compared to NTH (Figure 1E,F). Once fully cross-linked (30 min after the initiation of the crosslinking reaction) the hydrogel demonstrated a shear-thinning behavior, with its viscosity decreasing to liquid-like values when the shear stress was applied and then increasing again to solid-like values when shear stress was slowly lifted (Figure 1G; Figure S3, Supporting Information). Again, the shear-thinning behavior was not influenced by the plasma treatment (Figure 1H). Such viscosity versus shear stress curves mimic what happens when the average operating pressure is applied to a syringe to extrude the hydrogel. In other words, even when cross-linked alginate PTH could still be injected. This is advantageous from the perspective of clinical application, as already cross-linked PTH packaged in the single syringe would not require any additional preparation or handling skills. However, the viscosity of such recovered hydrogel was lower at 100 Pa·s, compared to 1000 Pa·s for the freshly cross-linked hydrogel. Importantly, the crosslinking had no effect on the cell viability. In other words, the hydrogel that was first fully cross-linked and then extruded on top of the cells with syringe had exactly the same effect on the cell viability as the injectable hydrogel (applied onto the cells as described in Figure 1A) – being non-cytotoxic when not treated with plasma (NTH) and cytotoxic when treated with plasma (PTH). The same was true when the non-cross-linked alginate was applied to the cells (Figure S4,

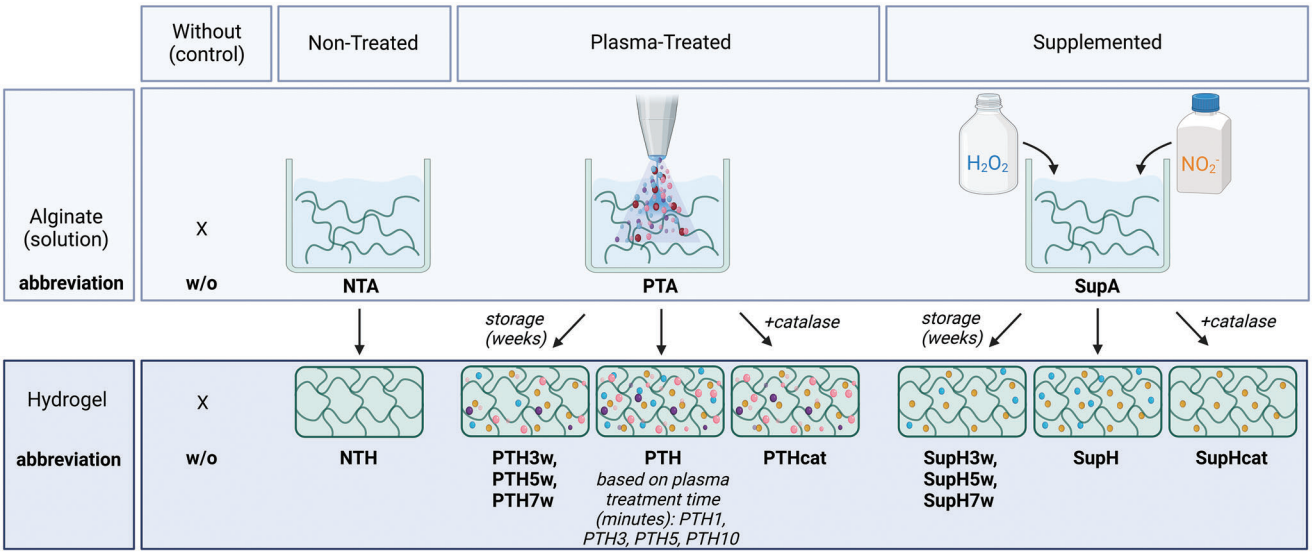

Figure 2. Overview of conditions and abbreviations used in this study.

Supporting Information). Finally, there were no obvious differences in the porous microstructure of NTH and PTH10 as observed by scanning electron microscopy (SEM) (Figure 1I). Taken together, we can conclude that plasma treatment did not alter any important physical properties of the alginate hydrogel.

Figure 2 provides an overview of different conditions and respective abbreviations used in the results section. We differentiate between non-cross-linked alginate solution ("A") and cross-linked alginate hydrogel ("H"). Depending on the treatment status of alginate, "A" and respective "H" can be: non-treated (NTA, NTH), plasma-treated (PTA, PTH) and artificially supplemented with H_2O_2 and NO_2^- solutions (SupA, SupH).

2.2. PTH for Delivery of Plasma-Derived RONS: RONS Generation, Release, and Aging

To investigate if PTH can be used as a vehicle for the delivery of plasma-derived RONS, two properties were studied: 1) concentration of RONS in PTA and 2) release of RONS from PTH. For this, first, the alginate solution was treated with plasma for 1–10 min and two biologically relevant long-lived RONS, hydrogen-peroxide (H_2O_2) and nitrite (NO_2^-) were quantified (**Figure 3A**). In addition, the presence of nitrates (NO_3^-) was also studied, as they are among the most relevant long-lived RONS alongside NO_2^- and H_2O_2. The results show a linear correlation between H_2O_2 concentration and plasma treatment time (R^2 = 0.950). However, there was a notable delay in H_2O_2 generation as observed by very low H_2O_2 concentrations for the 1-min plasma treatment time and the pronounced negative intercept in the linear regression line (Y = 103.2 × X-89.57). This suggests a certain degree of interaction between the alginate polymer chains and plasma that resulted in the slight scavenging of H_2O_2 visible at shorter plasma treatment times. Nevertheless, cytotoxic H_2O_2 concentrations could be reached in PTA. Similarly, the generation of NO_2^- in PTA correlated linearly with the plasma treatment time, although with a lower goodness-of-fit (R^2 = 0.90). The lag in NO_2^- production upon initiation of plasma treatment was not as evident (Y = 18.26 × X-12.08) as in H_2O_2. As a result, the H_2O_2:NO_2^- ratio varied significantly for different plasma treatment times, being 1.4 for 1 min and 5.3 for the 10 min treatment time. As plasma treatment is known to acidify liquids, the pH of PTA solutions was measured. Alginate acted as a buffer to stabilize the pH-value around neutral even for longer plasma treatment times (Figure 3B). This is relevant for the stability of RONS generated in PTA, as acidic pH favors reactions in which H_2O_2 in particular is depleted.

Next, PTA obtained by medium (5 min) or long (10 min) plasma treatment time, was cross-linked to a respective hydrogel (PTH5, PTH10), and the release of H_2O_2 and NO_2^- to the receptor medium was studied (Figure 3C,D). To observe if plasma treatment alters the alginate in a way that could influence the release of RONS, a control was included (SupH) where the hydrogel was prepared using alginate that was not treated with plasma but that was instead artificially supplemented with H_2O_2 and NO_2^- solutions (SupA). The release profile was identical for all three conditions (SupH, PTH5, and PTH10) with 75% of RONS released after 15 min and their complete release after 30 min. It appears that H_2O_2 was retained in the hydrogel slightly longer than NO_2^- reaching 50% of release after 10 min compared to 5 min for NO_2^-.

2.3. PTH Chemistry Is More than Just H_2O_2-Chemistry

PTA (treated for 5 min with plasma) and SupA (supplemented with [H_2O_2] and [NO_2^-] to match 5-min plasma treatment) solutions were stored at room temperature (RT) for up to 7 weeks and the stability or aging of H_2O_2 and NO_2^- molecules was studied. At weeks 0, 3, 5, and 7, the stored solutions were cross-linked to prepare aged PTH and SupH hydrogels, respectively, and treat osteosarcoma cell line MG63. This experiment had three related objectives: 1) to estimate the shelf-life of PTA/PTH, 2) to correlate the storage time of solution (PTA and SupA) and the

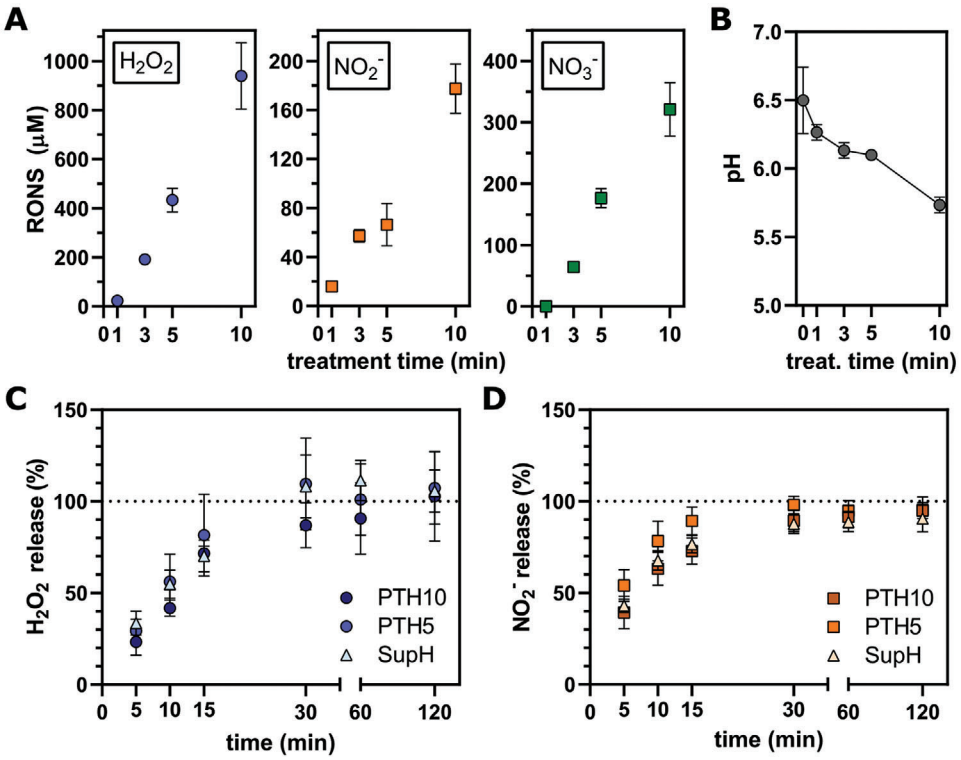

Figure 3. PTH as a vehicle for delivery of RONS: RONS generation and release. A) Concentration of H_2O_2, NO_2^-, and NO_3^- and B) pH-value of plasma-treated alginate solution (PTA) for different treatment times. C) Release of H_2O_2 and D) NO_2^- from the 5- or 10-min plasma-treated hydrogel (PTH5, PTH10) or from the hydrogel that was artificially supplemented with H_2O_2 and NO_2^- (SupH). Replicates were generated by three individual plasma treatments ($n = 3$). Each replicate was quantified minimum two times and the mean was calculated. Data is presented as mean ± SD.

remaining H_2O_2 concentration with the cytotoxicity of the respective hydrogel (PTH and SupH), and 3) to observe potential differences in aging and cytotoxicity between plasma-treated and supplemented samples that may indicate different chemical complexities (plasma chemistry vs H_2O_2-chemistry). Related to the objectives, an additional control condition was included, where catalase enzyme was added to the freshly made PTA and SupA to artificially deplete them of H_2O_2. These were then used to prepare PTHcat and SupHcat, respectively (see Figure 2).

The results show a significant difference in H_2O_2 aging for PTA and SupA, with slopes being 60 and 26, respectively ($R^2 \approx 0.9$) (**Figure** 4A). This means that after 7 weeks at RT, on average 0% of initial H_2O_2 concentration remained in PTA versus 83% in SupA. In contrast, NO_2^- was stable throughout the experiment (Figure 4B). The pH-values of PTA and SupA were similar and also stable for the duration of the experiment and, thus, could not be used to explain differences in H_2O_2 depletion rates of PTA and SupA (Figure 4C). The cytotoxicity or cell viability was largely dependent on the concentration of H_2O_2 left in stored PTA and SupA at the moment of the preparation of PTH and SupH (Figure 4D,E). However, there were some interesting observations made for PTH in particular. Namely, the duration of the aging experiment was just enough to obtain an H_2O_2-depleted PTH (PTH7w). As a result, the cytotoxicity of PTH7w was significantly reduced compared to freshly prepared PTH (PTH0w), with ≈80% of the cells surviving the PTH7w treatment. Nevertheless, this low cytotoxicity of PTH7w was still significantly higher (<0.01) than the cytotoxicity of PTHcat (also depleted of H_2O_2), where on average ≈95% of the cells survived the treatment, which was comparable to the negative control (NTH). This can be appreciated in the bottom right corner of Figure 4E (*pink and orange circles*). This observation further corroborates that the chemical complexity of PTH could not be reduced to simple H_2O_2 chemistry. In line with this, a similar observation was made when the cytotoxicity of PTH3w was compared to the cytotoxicity of PTH5w and SupH5w. All three hydrogels contained very similar concentrations of H_2O_2, yet only 10% of the cells survived PTH3w treatment compared to almost 60% of the cells that survived PTH5w or SupH5w treatment (Figure 4E). This may suggest the presence of other molecules besides H_2O_2 that contribute to the cytotoxicity of PTH and age differently.

2.4. PTH for Cancer Treatment: Cytotoxicity and Immunogenicity in Osteosarcoma

To demonstrate the application of PTH in cancer treatment, three different osteosarcoma cell lines (MG63, 143B, and SaOS2) were treated with PTH for 24, 48, or 72 h and cell viability was measured (**Figure** 5A–D; Figure S5, Supporting Information). To prepare PTH, three different plasma treatment times were used: 1, 3, or 5 min (PTH1, PTH3, PTH5). Expectedly, the cytotoxicity of PTH correlated with the plasma treatment time. The cytotoxicity of PTH could be attributed to the plasma-derived RONS, as NTH

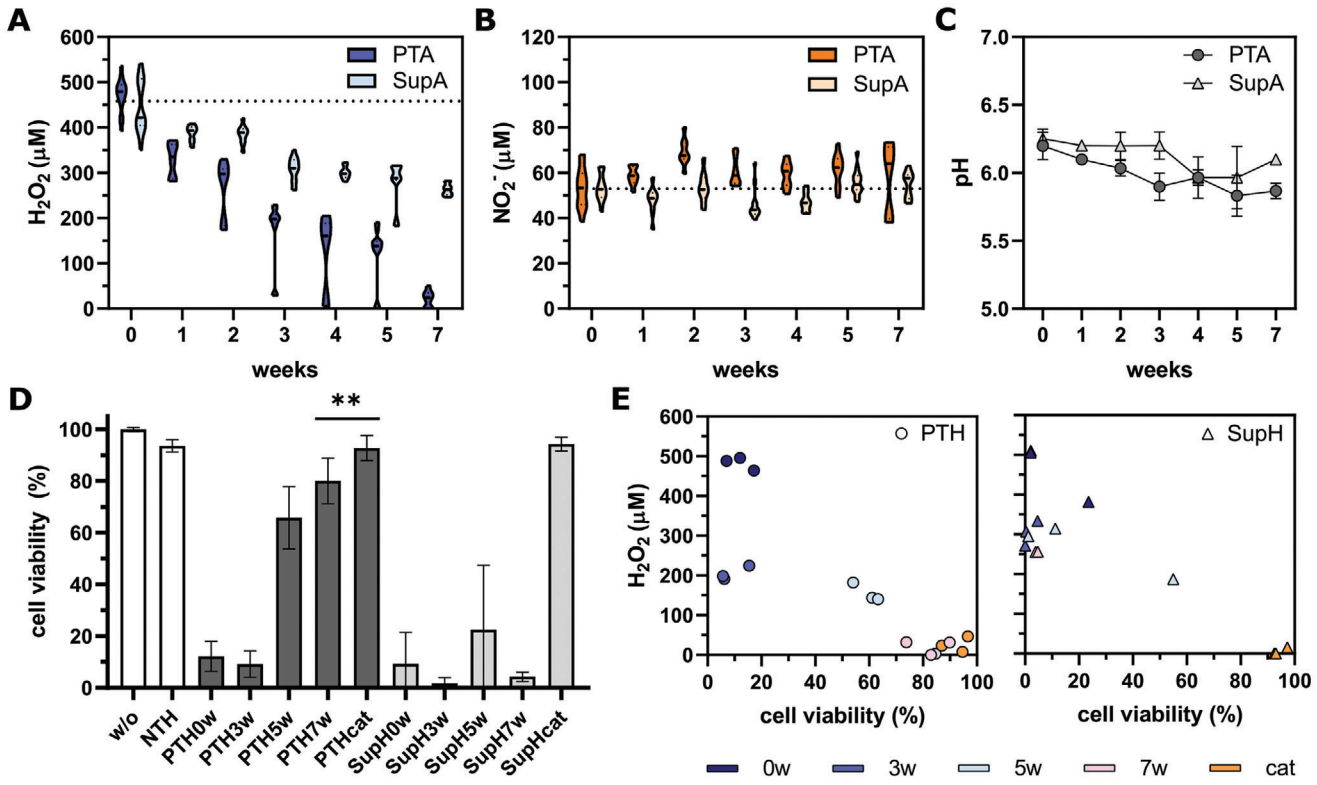

Figure 4. Aging of RONS and its effect on PTH cytotoxicity. A) Evolution of the H_2O_2 and B) NO_2^- concentration, and C) pH-value in PTA and SupA solutions that were stored at room temperature for 7 weeks, n ≥ 3. D) Cytotoxicity in MG63 of PTH and SupH hydrogels prepared using either freshly made (0w) or 3-,5- or 7-weeks stored PTA/SupA solutions. Three controls were used: no hydrogel (w/o), non-treated hydrogel (NTH), hydrogel where catalase enzyme was added to deplete H_2O_2 (PTHcat, SupHcat). t-test (<0.01**) was performed to compare cytotoxicities of PTH7w and PTHcat, as in these two conditions [H_2O_2] ≈0. E) Correlation between the cytotoxicity of PTH or SupH and their H_2O_2 concentration (that remained after 0–7 weeks of storage, or upon the addition of the catalase enzyme). Each dot represents an individual replicate.

(negative control) did not seemingly affect cell viability or proliferation. For short plasma treatment times (1 min), PTH cytotoxicity varied between the biological samples (*symbols of different colors in* Figure 5A–D). Generally, the majority of variability could be attributed to biological replicates, whereas technical replicates were highly reproducible (*symbols of the same color in* Figure 5A–D). For longer plasma treatment times (3 and 5 min), PTH treatment was not only more cytotoxic but also had a cytostatic effect, meaning that surviving cancer cells did not recover/proliferate further for the duration of the experiment. Different cell lines showed slightly different sensitivities to PTH treatment, with MG63 being the most resistant and cell lines with higher proliferative capacity (metabolism) (143B) and smaller cell size (SaOS2) being more sensitive.

We further investigated the immunogenicity of cell death by detecting the presence of two damage associated molecular patterns (DAMPs) that act as alarm signal to promote immune responses: secretion of high-mobility group box 1 protein (HMGB1) (Figure 5E) and translocation of calreticulin (CRT) protein to the cell surface (Figure 5F,G). CRT is known as "eat me signal" and CD47 receptor as its counterpart or "do not eat me signal" that protects cells from CRT-mediated phagocytic uptake. This receptor was not increased in response to the PTH treatment in MG53 and 143B cell lines and showed minimal increase in SaOS2 cell line compared to w/o control (Figure 5H). Immunogenicity was investigated only for the lowest plasma treatment time (1 min) as low cytotoxicity of PTH1 treatment allowed for a sufficient number of cells that survived and could be analyzed afterward. However, as it can be observed from Figure 5A–C, PTH1 showed very variable, and sometimes very low cancer cell cytotoxicity. This variability was also reflected in the expression of DAMPs, as DAMPs are released from dying cells. Despite this, enhanced expression of DAMPs could be observed. For HMGB1 we made an interesting observation that significantly less protein was present in the conditioned medium when cells were incubated with NTH compared to when cells were incubated without any hydrogel (w/o). We speculate that HMGB1 adhered to alginate hydrogels, so that the HMGB1 released could not be detected in its entirety by sampling the conditioned medium. In spite of this, there was still a significant increase in HMGB1 concentration upon PTH treatment compared to NTH control, indicating a pronounced immunogenic effect of the PTH treatment (Figure 5E). The expression of cell-surface CRT was unexpectedly increased both in PTH- and NTH-treated cells, although to a lesser extent in the latter (Figure 5F,G). Despite CRT being an eat-me signal for phagocytic cells, enhanced phagocytic uptake was observed only for PTH-treated and not for NTH-treated cancer cells when these cells were co-cultured with human monocyte-derived immature dendritic cells (iDCs) (**Figure** 6A,B). Notably, iDCs that were derived from different blood donors (*each donor*

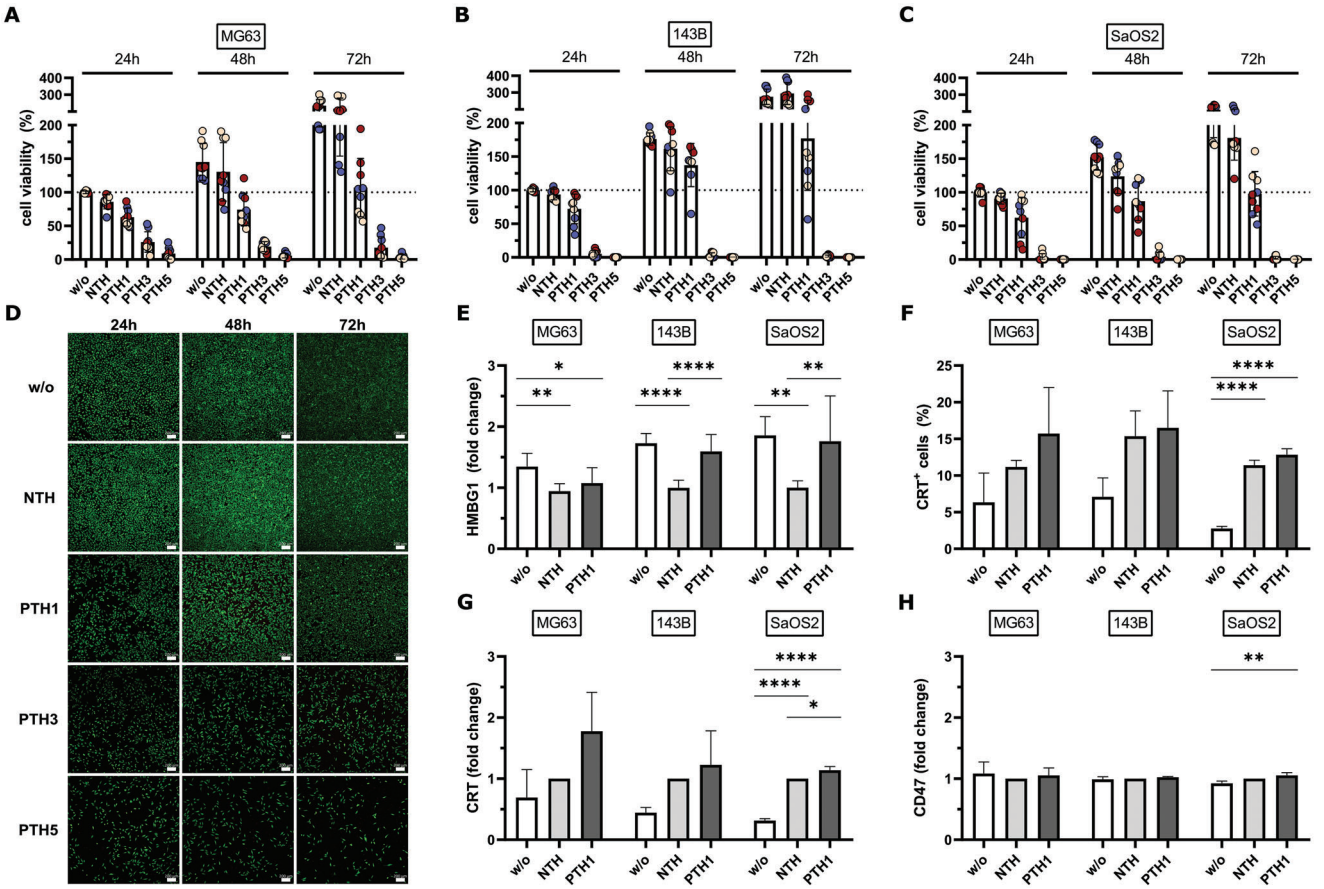

Figure 5. Cytotoxicity and immunogenicity of PTH treatment in osteosarcoma. A–C) Cell viability of three osteosarcoma cell lines after 24–72 h of treatment with 1-, 3-, or 5-min plasma-treated hydrogel (PTH1, PTH3, PTH5). Cells incubated without any hydrogel (w/o) or with non-treated hydrogel (NTH) were used as control. To observe proliferation, cell viability is given relative to control (w/o) at 24 h. Dots of different colors represent biological replicates and of same colors technical replicates. D) Confocal live/dead images for MG63 cell line (10x, scale bar 200 µm). Green dots represent live cells. E) Concentration of released HMGB1 protein in the conditioned medium at 24 h. F) Percentage of cells displaying calreticulin (CRT) on their surface at 24 h and G) CRT fold change at 24 h. H) CD47 fold change at 24 h. E–H) One way ANOVA (Tukey's multiple comparison test) was used to determine statistical significance ($p < 0.05^{*}$, $<0.01^{**}$, $<0.001^{***}$, and $<0.0001^{****}$), $n = 9$ for HMBG1 and $n = 3$ for CRT and CD47.

corresponds to one color in Figure 6) showed significant variation in their phagocytic capacities. For example, for blood donors labeled with dark blue color there were <10% of iDCs engulfing MG63 cells in the control condition, compared to 30% for blood donors labeled with red color. Regardless of the donor, PTH treatment consistently led to ≈1.5 times increase in phagocytosis for MG63 and SaOS2 cell lines. For the 143B cell line, the results were not as conclusive, with significant variations between the replicates. This may again be attributed to the fact that PTH1 treatment (used in the co-culture experiment) showed inconsistent cytotoxicity (see Figure 4B). In other words, the number of 143B cells affected by the PTH treatment might have been too low to drive more pronounced immunostimulatory effects. Besides phagocytotic capacity, co-cultured DCs were analyzed for different maturation markers (CD80, CD83, and CD86), indicative of their activation (Figure 6C–E). While the expression of CD80 and CD86 remained unchanged, CD83 marker significantly increased in SaOS2 cell line and showed a tendency toward increase in the other two cell lines. Again, the increase in CD83 marker coincided with the phagocytotic capacity of that particular blood donor. For example, for blood donors labeled in blue, there was a significant increase both in phagocytosis (Figure 6B) and CD83 expression (Figure 6C) in all three cell lines. This exemplifies how biological differences could impact the therapeutic outcome.

3. Discussion

While there have been a few reports on the cancer cytotoxicity of different PTHs,[24,25] so far, no study investigated the immunogenicity of the PTH treatment. Activation of the immune system is important for systemic and long-lasting therapeutic effects, and the ability of plasma to induce immunogenic cell death and promote anti-tumor immune responses has already been observed for direct plasma treatment and PTLs.[13,28] We demonstrated for the first time that these effects (release of danger signals and promoted phagocytosis) can also be achieved with PTH (Figures 5 and 6), establishing PTHs as a third plasma-treatment modality. Although PTHs have been proposed as an alternative to PTLs already a couple of years ago,[19] they still remained largely unexplored, as they require interdisciplinary expertise,

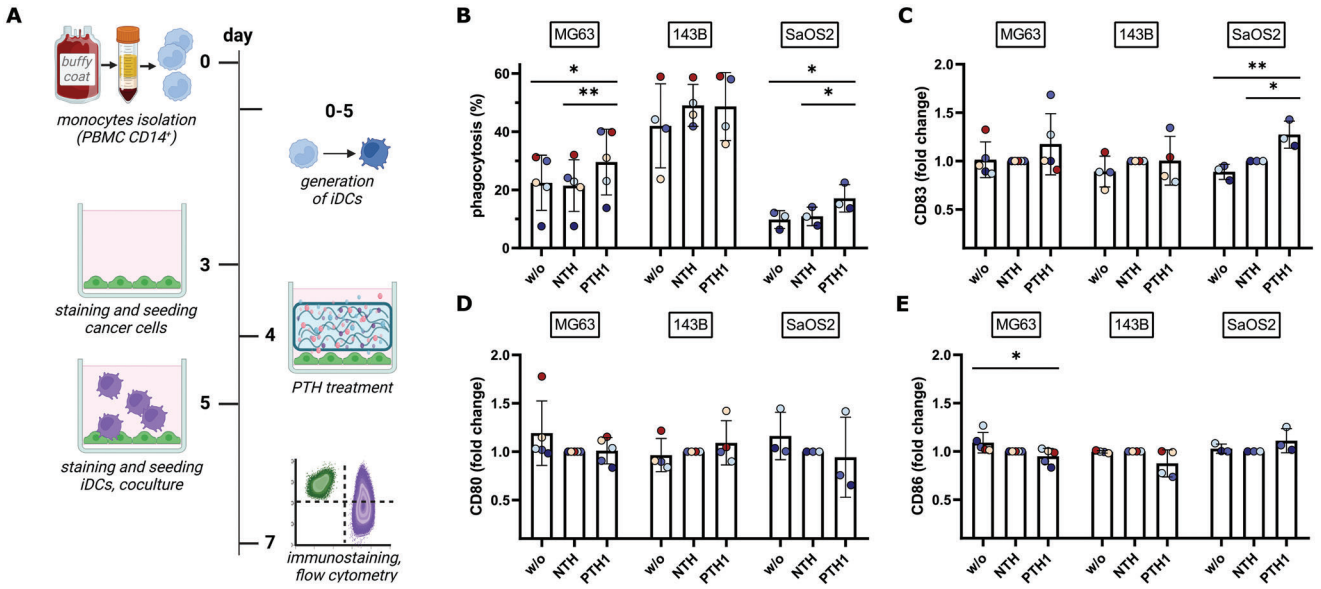

Figure 6. PTH treatment promoted phagocytic uptake of osteosarcoma. A) Timeline and workflow of co-culture experiment: generation of human monocyte-derived immature dendritic cells (iDCs) isolated from healthy blood donors, their co-culture with PTH-treated osteosarcoma cells (MG63, 143B, and SaOS2), and flow cytometry analysis. B) Percentage of phagocytic iDCs, and C–E) expression of three different DCs maturation markers after 48 h of co-culture. iDCs were co-cultured with osteosarcoma cells that were either not treated with any hydrogel (w/o), treated with non-plasma-treated hydrogel (NTH), or treated with 1-min plasma-treated hydrogel (PTH1). Linear mixed model followed by Tukey's HSD test was used to determine statistical significance ($p < 0.05^{*}$, $<0.01^{**}$, $<0.001^{***}$, and $<0.0001^{****}$), $n \geq 3$. Different colors represent different blood donors (total five donors).

combining biomedical engineering, (cancer) biology, and plasma physics and chemistry. In this context, we recently proposed a common 4-step (+ an iteration step) workflow for the development and characterization of PTH.[13] Here, we followed the proposed workflow, reporting results on 1) the hydrogel design, 2) the physical and 3) chemical compatibility of the hydrogel with plasma treatment, and 4) the biological effects of the hydrogel in context of cancer treatment.

3.1. Hydrogel Design

Some of the important design features of hydrogels for biomedical applications are biocompatibility, biodegradability, and crosslinking mechanism as it dictates hydrogel delivery route (injection or implantation).[30] The two studies that explored PTH for RONS-based cancer treatment, worked with thermosensitive polymers that gelate to hydrogel at body temperature, which allows for injectability at ambient temperature.[24,25] Here, we used a different strategy to produce an injectable PTH. We reported an optimized protocol that can be used to develop injectable and shear-thinning alginate-based PTH that could adapt to the shape of a cavity (Figure 1). Alginate hydrogels have physical properties similar to the extracellular matrix of different tissues. Thus, alginate is an important polymer in biomedical engineering, being explored for bio-inks and tissue engineering, drug delivery, and cell encapsulation.[26,27] It is a biocompatible and biodegradable natural polymer that is rather inert but can be easily modified or combined with further polymers to enhance its biological activity.[27] In other words, alginate hydrogels, therefore alginate PTH, could offer a great engineering basis and versatility in the context of different biomedical applications. It was previously described that when producing alginate PTH, the crosslinking of plasma-treated alginate (PTA) is a critical step. Namely, immersion of PTA in $CaCl_2$ crosslinking solution, led to a major loss of RONS through their washing out from the liquid hydrogel phase.[19] If, in contrast, $CaCl_2$ is added to PTA, parts of PTA that come in contact with $CaCl_2$ first, will cross-link immediately, while the rest will remain liquid, again leading to the loss of RONS. In this study, we adapted the crosslinking protocol to entirely preserve the RONS that have been generated in PTA (Figure 3C,D). More specifically, we cross-linked PTA by adding a small volume of a crosslinking mixture consisting of $CaSO_4$ crosslinking solution and Na_2HPO_4 retardant solution. $CaSO_4$ has lower solubility than $CaCl_2$ which results in slower Ca^{2+} release and a more controlled crosslinking reaction. Additionally, phosphate groups in the retardant solution compete with carboxylate groups in alginate for Ca^{2+}, which slows down the crosslinking reaction even further.[26,31] By adjusting the concentration of crosslinking and retardant solutions, we obtained a hydrogel that crosslinks slow enough to allow for injectability, yet fast enough to prevent dilution of material upon injection in a liquid (Figure 1B; Figure S1, Supporting Information). Moreover, such controlled crosslinking allowed for hydrogels that can adapt the shape to the form of any (dry) cavity (Figure 1C; Figure S2, Supporting Information). These properties are important for two potential applications of PTH: 1) PTH injection for non-surgical (minimally invasive) and high local delivery of RONS to internal tumors that cannot be resected, and 2) PTH injection for post-surgical treatment (after surgical resection of the tumor) to fill in the cavity and treat surgical margins/prevent local cancer recurrence. It is important to note that the crosslinking protocol for

PTA, specifically the concentrations of crosslinking and retardant solutions, may have to be adapted if different alginate is used. Namely, commercially available alginates differ in their molecular weight as well as the ratio and distribution of the polymer building blocks, β-D-mannuronate (M) and α-L-guluronate (G). Since G units are mainly responsible for the crosslinking of alginate as they form ionic bonds with divalent cations, alginates with different G content may gelate differently and lead to different physical properties of the hydrogel for the same crosslinking conditions.[32]

3.2. Physical and Chemical Properties

Plasma treatment did not impair the ability of alginate to form a hydrogel nor did it change the rheological properties of the alginate hydrogel (Figure 1D–H). Plasma treatment led to treatment-time-dependent generation of biologically important long-lived RONS,[33] H_2O_2 and NO_2^-, in alginate (Figure 3A). While the correlation between the treatment time and H_2O_2 concentration was linear, the H_2O_2 generation was notably slow at the beginning of the plasma treatment, implying some sort of (scavenging) chemical interaction between alginate polymer and plasma. This is in line with our previous results where the same plasma device was used (kINPen) to treat alginate. This effect was even more visible when alginate was treated with a different plasma source (another APPJ device), where detectable H_2O_2 concentrations were reached only after 45 s of treatment.[19] By comparing the release of RONS from PTH with that of artificially supplemented hydrogel (SupH) we could show that plasma did not induce any physicochemical alterations in alginate that may impact the full release of RONS (Figure 3C,D), so alginate is compatible with plasma in the context of RONS delivery.

Interestingly, H_2O_2 aged/degraded at a significantly faster rate in PTA than in SupA, with 100% degradation after 7 weeks at RT for PTA versus only 17% for SupA (Figure 4A). H_2O_2 is known to degrade faster at more acidic pH-values.[9] However, the pH was around neutral and the same for both PTA and SupA (Figure 4C). These results suggest that the chemical properties of alginate upon plasma treatment cannot be mimicked by supplementing alginate with H_2O_2/NO_2^- solutions. A recent publication provides a mechanistic insight supported by computational and experimental data on how plasma may be interacting with alginate to introduce different chemical modifications.[22] In their study, the authors report the possible formation of different organic peroxides and intermediate products as the result of plasma oxidation of alginate. Nevertheless, it is a different research question to which extent these chemical modifications have a biological effect. While it is clear that H_2O_2 is the main cytotoxic component in chemically simple PTLs, as the depletion of H_2O_2 using catalase also eliminated the cytotoxic effect,[34] several studies reported that the cytotoxicity achieved with a PTL could not be entirely reproduced by supplementing that same liquid with H_2O_2/NO_2^-, implying the presence of further biologically relevant molecules.[18,34,35] Biological effects beyond H_2O_2-mediated cytotoxicity are more likely for chemically more complex liquids, for example, containing organic molecules.[17,18] These are yet unexplored for PTHs. In all, PTH showed stability up to 3 weeks, which is a very interesting timeframe stability of RONS is a crucial parameter in PTH, so this is an important issue to take into account whenever designing PTH for future translation to the clinics.

As PTHs are prepared by treating organic polymeric solutions, more complex plasma chemistry is expected for PTHs than PTLs. However, so far, no study aimed to investigate non-H_2O_2 mediated biological effects for PTH. Here, we tackled this research question as part of the "RONS aging" experiment (Figure 4). Namely, we generated H_2O_2-free PTH in two different ways: 1) by storing PTA for 7 weeks at RT, or 2) by adding catalase enzyme to freshly prepared PTA. While the latter resulted in a non-cytotoxic PTH (comparable to NTH control), the first preparation method preserved the cytotoxicity of PTH killing 20% of MG63 cells on average. From these results it could be concluded that although the catalase is considered highly specific for H_2O_2, its addition may also impact further molecules that contribute to the cytotoxicity of alginate PTH. The presence of cytotoxic components (with variable aging time) other than H_2O_2 was also implied when the cytotoxicity of PTH that was stored for 3 weeks was compared to the cytotoxicity of PTH and SupH stored for 5 weeks. While PTH3w had a very similar H_2O_2 concentration to PTH5w and SupH5w, its cytotoxicity was 95% as compared to only 45% for PTH5w and SupH5w (Figure 4E). Despite the interesting result, this experiment is limited with only few datapoints where H_2O_2 concentrations were similar enough to directly compare their cytotoxicities. In particular, H_2O_2 concentration in SupH remained very high (83% of the initial value) throughout the duration of the experiment (7 weeks), making direct comparison between PTH and SupH difficult. Thus, to be able to draw statistically significant conclusions, more data from longer experiments should be collected in the future. Furthermore, our study was limited to only studying cell cytotoxicity in global and without distinguishing different types of cell death (including immunogenic cell death). More in depth research is necessary to explore and attribute specific biological effects of PTH treatment to molecules other than H_2O_2.

3.3. Biological Effects and Potential Application

PTH treatment induced release of immunogenic signals in different osteosarcoma cell lines, as observed by HMGB1 release and translocation of CRT to the cell surface. CD47, as counterpart to CRT that can inhibit CRT-mediated phagocytosis, was not significantly increased. Interestingly, HMGB1 that was released from the cells appeared to adhere to the hydrogel (Figure 5E). This could possibly help maintain high local concentrations of HMGB1 immunogenic signal in vivo. In co-culture, PTH-treated osteosarcoma cells enhanced the phagocytic capacity of monocyte-derived iDCs (Figure 6A,B). The absolute phagocytic capacity was very different for different blood donors from which these immune cells were isolated. This exemplifies biological variability of people and its relevance for therapeutic responses, as phagocytic uptake of antigens is the first step in the cancer-immunity cycle that leads to specific and systemic T-cell mediated immunity.[29] After coming in contact with antigens and other danger or inflammatory signals, immature phagocytic DCs begin their maturation and migration toward T-cell-containing lymph nodes. Maturation is accompanied by

phenotypical changes such as the expression of co-stimulatory signals on the cell surface.[36] Upon 48 h of co-culture with PTH1-treated osteosarcoma cells, iDCs showed enhanced expression only for CD83 maturation marker, and no change in CD80 and CD86 markers. Later analysis time points may be needed to allow for the expression of these receptors to take place. It also needs to be mentioned that for ICD and co-culture experiments we have chosen to treat osteosarcoma cells with PTH1 (the lowest plasma-treatment time of 1 min) for the simple reason of having enough cancer cells that survive the treatment and can be analyzed afterward. However, the PTH1 treatment showed high variability in cell death between biological replicates (Figure 4A–C) that likely also impacted the variability in the expression of ICD markers and co-culture results. Related to this, 1-min treatment time may also be too short for biologically relevant oxidations to occur or accumulate in alginate.[22] It would be interesting to explore in the future if higher plasma treatment times lead to alginate PTHs with more pronounced (and non-H_2O_2-mediated) biological effects.

Our study represents not only the first report on immunogenicity of a PTH treatment, but also explores immunogenicity of plasma treatment (direct or indirect) in osteosarcoma for the first time. Osteosarcoma is known to be an aggressive and metastatic cancer that is rarely researched and has poor prognosis and treatment options. (Osteo)sarcomas often show resistance to therapies, so it would be interesting to see if they could acquire one also to the PTH treatment. This was already observed for melanoma and direct plasma treatment.[37] While intraosseous injections are difficult and limb amputation is a common procedure in patients with osteosarcoma, PTHs could be useful as post-operative treatment. Alginate-based PTH is especially interesting for applications in Ca^{2+}-rich bone environment that may allow for the in-situ crosslinking of the alginate. For example, sometimes a limb-sparing surgery is performed accompanied by the eventual implantation of a bone graft to promote regeneration of the tissue. In this context, we have already shown that a PTH could safely be combined with a calcium-phosphate implant for critical bone defects in rabbits.[38] Incorporating PTH in a bone graft could not only be significant for the treatment of surgical margins to kill any remaining cancer cells and prevent cancer recurrence, but also could improve the viscoelasticity of the graft. Furthermore, in rare cases an extraskeletal osteosarcoma can be formed outside of the bone. This cancer is histologically indistinguishable from osteosarcoma but is formed in soft-tissue. As for any soft-tissue sarcoma, the typical procedure is a wide resection of the tumor and the surrounding tissue.[39] Therefore, it is imaginable to apply our alginate PTH for postoperative treatment in soft-tissue sarcomas to prevent local cancer recurrence and fill in the cavity, which given the porous microstructure and viscoelastic hydrogel properties might also help tissue heal. This, however, remains the topic of further research that will require the use of animal models.

4. Conclusion

We developed and characterized an injectable and shape-adaptable alginate PTH for RONS-based cancer treatment. Thanks to its properties and versatility, alginate is an important polymer in biomedical engineering, making alginate-based PTH a prospective research field. Our PTH could release RONS within 30 min of the injection to kill osteosarcoma cells and induce release of immunogenic signals enhancing their phagocytic uptake by human monocyte-derived dendritic cells. This is the first study to demonstrate the immunogenicity of PTH treatment, consolidating PTH as third plasma-treatment modality and providing rationale for exploration of combinatorial treatment strategies.

5. Experimental Section

Cell Culture: Human osteosarcoma cell lines MG63 (ATCC CRL-1427) and 143B (ATCC CRL-8303) were cultured in DMEM (Thermo Fisher Scientific 10 313 021) supplemented with 10% FBS, 1% Penicillin/Streptomycin, and 2 mM L-Glutamine (complete DMEM). Human osteosarcoma cell line SaOS2 (ATCC HTB-85) was cultured in McCoy's 5A Medium (Thermo Fisher Scientific 16 600 082) supplemented with 10% FBS and 1% Penicillin/Streptomycin. Complete DMEM without Sodium-Pyruvate (Thermo Fisher Scientific 31 053 028) was used to seed cancer cells and in all experiments, as Sodium-Pyruvate is known to scavenge RONS.[40] Human PBMC-isolated monocytes and monocyte-derived immature dendritic cells (iDCs) were cultured in 1640 RPMI medium (ATCC 30–2001) supplemented with 2.5 % human AB serum (Sanbio A25761). This medium was also used to co-culture iDCs with cancer cells. To collect cells, TrypLE enzyme (Thermo Fisher Scientific 12 605 010) was used for cancer cells and PBS (Capricorn Scientific PBS-1A) with 1 mM EDTA was used for iDCs.

Plasma Treatment and Preparation of Hydrogels: To prepare injectable alginate hydrogels, three solutions prepared in sterile deionized water were used: 0.5% (w/v) sodium alginate solution (A0.5) (PanReac A3249), 1 M $CaSO_4{\cdot}2H_2O$ cross-linker solution (CS) (Merck 1 021 610 500), and 125 mM $Na_2HPO_4{\cdot}2H_2O$ retardant solution (RS) (Fluka BioChemika 71 644). First, CS and RS were mixed in a volume ratio 1:1 (e.g., 20 µL + 20 µL). Immediately after mixing them, this CS/RS mixture was transferred to the Eppendorf tube containing A0.5 solution in 1:10 volume ratio (e.g., 20 µL CS/RS + 200 µL A0.5) to initiate crosslinking reaction and obtain alginate hydrogel. The tube was flicked to mix well the solution and alginate hydrogel (e.g., 200 µL) was pipetted immediately onto the dry well plate (with or without cells). One minute later, 1 mL of liquid (water for RONS release experiment or cell culture medium for other experiments) was added on top of the hydrogel. To prepare plasma-treated hydrogels (PTH1, PTH3, PTH5, or PTH10), A0.5 was first treated for 1, 3, 5, or 10 min with a commercial kINPen IND device (NEOPLAS Tools) operated with high-purity argon gas (Air Liquide). In the main text, this is referred to as plasma-treated alginate (PTA). The treatment was done on 1 mL A0.5 in a 24-well plate at 1.1 slm gas flow rate, 10 mm distance, room temperature, and under a sterile hood. For non-treated hydrogel (NTH), non-treated A0.5 was used. For supplemented hydrogel (SupH), A0.5 was not treated with plasma, but only supplemented with Hydrogen Peroxide (H_2O_2) and Sodium nitrate (NO_2^-) (Sigma–Aldrich 563 218) (SupA) to match concentrations of respective PTA.

Rheology and SEM: Hybrid Rheometer Discovery HR-2 (TA Instruments) was used to study the rheological properties of the hydrogel. Following properties were measured: 1) storage (G') and loss (G'') modulus in function of time and 2) viscosity in function of shear stress. For this, CS/RS solution was added to alginate (treated or not treated with plasma) to start the crosslinking reaction. Immediately, 200 µL of this mixture was pipetted on the rheometer platform and the measurement was initiated. All measurements were done using a 20 mm flat plate geometry at a gap of 450 µm and room temperature. For the first 30 min, time sweep oscillatory measurements were performed at 1 Hz angular frequency, 3 s delay time, 1.10^{-3} rad displacement and G' and G'' were followed over time. After 30 min, rotational measurements were conducted to evaluate the shear thinning behavior and recovery of the cross-linked hydrogel. To this end, the viscosity of the hydrogels was monitored throughout an

increasing shear rate sweep from 0.1 to 100 Hz, followed by a second decreasing sweep from 100 to 0.1 Hz. To perform scanning electron microscopy (SEM), hydrogel was frozen using liquid nitrogen and then dried (Noxair lyophilizer). The sample was coated with a thin layer of gold and the morphology and topography of the microstructure of hydrogel was examined using Zeiss Neon40 field emission SEM.

RONS and pH Quantification: Nitrite ions (NO_2^-) were quantified using the Griess test. Griess reagent was prepared by dissolving 0.1% (w/v) of N-(1-naphthyl) ethylenediamine dihydrochloride, 1% (w/v) of sulphanilamide, and 5% (w/v) of phosphoric acid in deionized water. To quantify NO_2^-, 50 µL of sample was transferred to a transparent 96-well plate and 50 µL of Griess reagent was added on top and mixed well. Absorbance was measured at $\lambda = 540$ nm using a Synergy HTX Hybrid Multi Mode Microplate Reader (BioTek Instruments, Inc.). A calibration curve prepared in 0.5% alginate was used to calculate the NO_2^- concentrations from the absorbance values. Hydrogen peroxide (H_2O_2) was quantified using Amplex Red/Horseradish peroxidase (AR/HRP)-based fluorescence assay (Sigma). To quantify H_2O_2, the sample was first diluted in deionized water 1:100 (for plasma-treatment times of 1 and 3 min) or 1:200 (for plasma-treatment times of 5 and 10 min). Then, 200 µL of the diluted sample was transferred to a black 96-well plate and 50 µL of AR/HRP solution was added on top and mixed well. The plate was incubated for 30 min at 37 °C and in the dark. Fluorescence was measured for $\lambda_{ex} = 560/20$ nm and $\lambda_{em} = 590/20$ nm using a Synergy HTX Hybrid Multi Mode Microplate Reader (BioTek Instruments, Inc.). Since two different dilutions were used, two different calibration curves were necessary to calculate the H_2O_2 concentrations from fluorescence values (prepared in 0.5% alginate solution diluted 100 or 200 times). Nitrates (NO_3^-) were quantified using a Nitrate Test Spectroquant kit (Sigma–Aldrich, 1.09713.002), following the manufacturer's protocol. Prior to NO_3^- quantification, NO_2^- was removed by adding 5 µL of sulfamic acid to the sample (final concentration 2 mM). The calibration curve was obtained using KNO_3 standard solutions in 0.5% alginate solution. The absorbance value at 330 nm was used to calculate the concentration of NO_3^-. pH was measured using pH strips (2.0–9.0) with automated reader device (Macherey-Nagel 92 118).

RONS Release: To study the release of NO_2^- and H_2O_2 from hydrogel, 200 µL of hydrogel were pipetted onto a 24-well plate and 1 min later, 1 mL of deionized water was added on top. The plate was incubated at 37 °C and after 5, 10, 15, 30, 60, 120, and 180 min, 50 µL of water was collected from the well for the detection of released NO_2^- by Griess test, and 25 µL of water was collected and diluted 1:100 for the detection of released H_2O_2 by AR/HRP assay. At each time point, 75 µL of fresh deionized water was added to the well to compensate for the collected volume. In this experiment, RONS release was studied for three different hydrogels: PTH5, PTH10, and SupH. These hydrogels were prepared by treating 0.5% alginate solution with plasma for 5 or 10 min, or by supplementing alginate solution with 1M H_2O_2 and 0.2 M NO_2^- (concentrations that roughly correspond to the plasma-treatment time of 10 min). Initial RONS concentration ("100%") was quantified from non-cross-linked alginate solutions (PTA5, PTA10, or SupA).

Cytotoxicity: Cancer cells were seeded in a 24-well plate in complete DMEM without Sodium-Pyruvate 18 h before treatment (40 000 cells well^{-1}). To treat cells, the conditioned cell culture medium was removed from the well and 200 µL of hydrogel was injected directly onto the cells. One minute later, 1 mL of fresh complete DMEM without Sodium-Pyruvate was added on top. For each condition, three technical replicates were performed. After 24, 48, or 72 h, the hydrogel and conditioned medium were removed and Presto Blue cell viability reagent was added to the cells (250 µL well^{-1} of 1:10 dilution in cell culture medium; Thermo Fisher Scientific P50200). The cells were incubated for 1 h with Presto Blue, after which the reagent was transferred to a black 96-well plate (100 µL well^{-1}) and the fluorescence was measured ($\lambda_{ex} = 560$ nm, $\lambda_{em} = 590$ nm). For microscopy, the remaining Presto Blue was removed from the cells, the cells were washed with 1 × PBS and live/dead stain (Thermo Fisher Scientific L3224) was added to the cells for microscopy imaging according to the manufacturer's protocol.

Expression of ICD Markers: To study the expression of immunogenic cell death (ICD) markers, cancer cells were seeded in a 6-well plate in DMEM without Pyruvate 18 h before the PTH treatment (200 000 cells well^{-1}). To treat cells the conditioned cell culture medium was removed and 1 mL of hydrogel was injected directly onto the cells. One minute later, 5 mL of fresh complete DMEM without Sodium-Pyruvate was added on top. After 24 h, the cells were analyzed for the secretion of high mobility group box 1 (HMGB1) protein and the presence of calreticulin (CRT) and CD47 surface receptors. For the quantification of HMGB1, 10 µL of the conditioned medium was collected and HMGB1 Express ELISA (IBL International/Tecan 30 164 033) was performed according to the manufacturer's protocol. For the receptor analysis, the cells were collected and stained for flow cytometry. For CRT, Alexa Fluor 488 Anti-Calreticulin antibody (Abcam Ab196158) and Alexa Fluor 488 Rabbit IgG isotype control (Abcam Ab199091) were used in combination with PI viability staining (Merc, P4170-25MG). For CD47, PE Mouse Anti-human CD47 antibody (BD Bioscience 556 046) and PE Mouse IgG1 κ isotype control (BD Biosciences, 555 749) were used in combination with DAPI viability staining. 25 000 events were acquired. The cells were gated for live and single cells. Mean fluorescence intensity (MFI) was used to calculate the fold change in the cell receptor expression. The overtone function (FlowJo software) was used to obtain the percentage of CRT^+ cells.

Generation of Immature Dendritic Cells: Human peripheral blood mononuclear cells (PBMCs) were isolated from a buffy coat fraction of whole blood donations by healthy adult volunteers (provided by Red Cross Flanders Blood service, Belgium). To isolate PBMCs, 25 mL of the buffy coat was added to a Falcon tube containing 15 mL Lymphoprep density gradient medium (Stemcell technologies) without mixing the two solutions. The tube was spun down using a swing-out rotor at break 0 and the distinct PBMCs band was transferred to a new Falcon tube and washed two times with 1 × PBS containing 1 mM EDTA. PBMCs count and the percentage of monocytes were determined using the Abx Micros 60 hematology analyzer (Horiba). Monocytes were then isolated from PBMCs using a CD14 magnetic activated cell sorting (MACS) (Miltenyi Biotec 200-070-118): Pelleted PBMC were resuspended in MACS buffer (800 µL per 100 × 10^6 cells) and incubated with CD14 microbeads (200 µL per 100 × 10^6 cells) for 15 min at 4 °C. The cells were washed with MACS buffer and loaded onto the equilibrated MACS column placed on the magnet. The column was washed three times to remove the cells that did not bind. The column was then removed from the magnet and $CD14^+$ cells (monocytes) were collected into the new Falcon tube with 5 mL MACS buffer. Collected monocytes were washed with 1640 RPMI medium to remove MACS buffer and cultured in 1640 RPMI medium supplemented with 2.5 % human AB serum at cell density 1.2 × 10^6 cells mL^{-1}. To obtain immature dendritic cells (iDCs), 800 IU mL^{-1} granulocyte-macrophage colony-stimulating factor (GM-CSF; Miltenyi Biotec 130-095-372) and 20 ng mL^{-1} interleukin (IL)−4 (Miltenyi Biotec 130-093-917) were added to the monocytes cell culture (day 0). iDCs were harvested on day 5. For positive control, a maturation cocktail was added to iDCs on day 5: 20 ng mL^{-1} tumor necrosis factor alpha (TNF-α; Miltenyi Biotec 130-094-017) and 1 µg mL^{-1} prostaglandin E2 (PGE2; Bio-Techne Ltd 2296). Mature dendritic cells (mDCs) were harvested on day 7.

Co-Culture Experiments: For co-culture experiments, cancer cells were stained with PKH-67 dye (1 µL per 1 × 10^6 cells) following the manufacturer's protocol (Sigma-Aldrich MINI67) and seeded in a 6-well plate (100 000 cells/plate) in complete DMEM without sodium pyruvate 18 h before the treatment. On the next day, cancer cells were treated with hydrogel. Twenty-four hours later, hydrogel was removed and cancer cells were co-cultured with iDCs. For this, iDCs were first collected and stained with CellTracker Violet BMQC dye (0.2 ul of 10 mM dye per 1 × 10^6 cells; ThermoFisher Scientific C10094). Then the iDCs were seeded on top of the cancer cells in effector-to-target ratio 1:1. To know the number of iDCs that needed to be seeded, extra wells were used to count cancer cells that remained after the treatment. For iDCs seeding and co-culture 1640 RPMI medium supplemented with 2.5 % human AB was used. Cells were co-cultured for 48 h before they were collected and immunostained for flow cytometry analysis (200 000 cells/staining, total four stainings): full fluorescence (CD80, CD83, and CD86) and three fluorescence-minus-one (FMO) controls. Following antibodies were used: anti-CD80-PerCPCv5.5 (Biolegend 400 150), anti-CD83-APC (BD Biosciences 551 073), and

anti-CD86-PE-Cv7 (Y) (BD Biosciences 557 872). Unstimulated monocytes were used as negative control and mDC as the positive control. DC events (20 000) were acquired at Novocyte Quanteon flow cytometer. Cells were gated for single cells and live cells and mean fluorescence intensity (MFI) for each CD maturation marker was reported and used to calculate fold change. The percentage of phagocytotic DC cells was calculated as PHK-67$^+$ AmCyan$^+$ cells divided by AmCyan$^+$ cells.

Statistical Analysis and Figures: All data is presented as mean ± SD. Statistical significance was determined using a one-way analysis of variance (ANOVA) followed by Tukey's multiple comparisons test (95% confidence) (Prism Graph Pad). For co-culture experiments, to account for differences between immune cell donors (random variable), a linear mixed model followed by Tukey's HSD test was used (JMP software). Statistical significance was noted when $p < 0.05^*$ ($<0.01^{**}$, $<0.001^{***}$, and $<0.0001^{****}$). Figures were created using Prism GraphPad, Biorender, and Inkscape.

Supporting Information

Supporting Information is available from the Wiley Online Library or from the author.

Acknowledgements

The authors acknowledge Francesco Tampieri for constructive discussions related to polymers and plasma chemistry. The authors acknowledge Instituto de Salud Carlos III (ISCIII) and Next Generation EU funds through Project IHRC22/00003 SELLO EXCEL. ISCIII-HEALTH and MINECO for PID2019- 103892RB-I00/AEI/10.13039/501100011033 and EUR2022-134060 / AEI / 10.13039/501100011033. M.Z., A.E., and C.C. belong to the SGR2022-1368. Support for the research of CC was received through the ICREA Academia Award for excellence in research, funded by the Generalitat de Catalunya. The authors thank also COST Action CA20114 (Therapeutical Applications of Cold Plasmas) for the stimulating environment provided. This work was partially funded by the Research Foundation—Flanders (FWO) and supported by the following Grants: 1S67621N (H.V.), 12S9221N (A.L.), and G044420N (A.B. and A.L.).

Conflict of Interest

The authors declare no conflict of interest.

Author Contributions

M.Z., A.E.N., A.L., and C.C. performed conceptualization. M.Z. and A.E.N. performed experimental work. M.Z., A.E.N., H.V., and C.C. performed the methodology. M.Z. and A.L. performed data curation. A.E.N., A.L., A.B., C.C., and E.S. performed supervision. M.Z. wrote the original draft. All co-authors wrote the review and contributed editing.

Data Availability Statement

The data that support the findings of this study are available from the corresponding author upon reasonable request.

Keywords

drug delivery, immunogenic cell death, injectable hydrogels, osteosarcoma, plasma medicine

Received: September 29, 2023
Revised: November 9, 2023
Published online:

[1] D. Yan, J. H. Sherman, M. Keidar, *Oncotarget* **2017**, *8*, 15977.
[2] T. Bernhardt, M. L. Semmler, M. Schafer, S. Bekeschus, S. Emmert, L. Boeckmann, *Oxid. Med. Cell Longev.* **2019**, *3*, 3873928.
[3] Z. Chen, G. Chen, R. Obenchain, R. Zhang, F. Bai, T. Fang, H. Wang, Y. Lu, R. E. Wirz, Z. Gu, *Mater. Today* **2022**, *54*, 153.
[4] D. Yan, Q. Wang, A. Malyavko, D. B. Zolotukhin, M. Adhikari, J. H. Sherman, M. Keidar, *Sci. Rep.* **2020**, *10*, 11788.
[5] H. Sies, D. P. Jones, *Nat. Rev. Mol. Cell Biol.* **2020**, *21*, 363.
[6] X. Lu, G. V. Naidis, M. Laroussi, S. Reuter, D. B. Graves, K. Ostrikov, *Phys. Rep.* **2016**, *630*, 1.
[7] E. Wu, L. Nie, D. Liu, X. Lu, K. (.K.). Ostrikov, *Free Radic. Biol. Med.* **2023**, *198*, 109.
[8] E. J. Szili, S.-H. Hong, J.-S. Oh, N. Gaur, R. D. Short, *Trends Biotechnol.* **2018**, *36*, 594.
[9] A. Khlyustova, C. Labay, Z. Machala, M.-P. Ginebra, C. Canal, *Front. Chem. Sci. Eng.* **2019**, *13*, 238.
[10] Y. Gorbanev, A. Privat-Maldonado, A. Bogaerts, *Anal. Chem.* **2018**, *90*, 13151.
[11] M. L. Semmler, S. Bekeschus, M. Schäfer, T. Bernhardt, T. Fischer, K. Witzke, C. Seebauer, H. Rebl, E. Grambow, B. Vollmar, J. B. Nebe, H.-R. Metelmann, T. V. Woedtke, S. Emmert, L. Boeckmann, *Cancers* **2020**, *12*, 269.
[12] L. Zhou, Z. Zhang, Z. Huang, E. Nice, B. Zou, C. Huang, *Mol. Biomed.* **2020**, *1*, 4.
[13] M. Zivanic, A. Espona-Noguera, A. Lin, C. Canal, *Adv. Sci.* **2023**, *10*, e2205803.
[14] H. Tanaka, S. Bekeschus, D. Yan, M. Hori, M. Keidar, M. Laroussi, *Cancers* **2021**, *13*, 1737.
[15] E. J. Szili, J.-S. Oh, S.-H. Hong, A. Hatta, R. D. Short, *J. Phys. D: Appl. Phys.* **2015**, *48*, 202001.
[16] A. Lin, E. Biscop, C. Breen, S. J. Butler, E. Smits, A. Bogaerts, *Oxid. Med. Cell Longev.* **2020**, *2020*, 9750206.
[17] F. Tampieri, Y. Gorbanev, E. Sardella, *Plasma Process. Polym.* **2023**, *20*, e2300077.
[18] H. Tanaka, S. Maeda, K. Nakamura, H. Hashizume, K. Ishikawa, M. Ito, K. Ohno, M. Mizuno, Y. Motooka, Y. Okazaki, S. Toyokuni, H. Kajiyama, F. Kikkawa, M. Hori, *Plasma Processes Polym.* **2021**, *18*.
[19] C. Labay, I. Hamouda, F. Tampieri, M.-P. Ginebra, C. Canal, *Sci. Rep.* **2019**, *9*, 16160.
[20] Y. Sun, D. Nan, H. Jin, X. Qu, *Polym. Test.* **2020**, *81*, 106283.
[21] R. D. Kasai, D. Radhika, S. Archana, H. Shanavaz, R. Koutavarapu, D.-Y. Lee, J. Shim, *Int. J. Polym. Mater. Polym. Biomater.* **2023**, *72*, 1059.
[22] F. Tampieri, A. Espona-Noguera, C. Labay, M.-P. Ginebra, M. Yusupov, A. Bogaerts, C. Canal, *Biomater. Sci.* **2023**, *11*, 4845.
[23] C. Labay, M. Roldán, F. Tampieri, A. Stancampiano, P. E. Bocanegra, M.-P. Ginebra, C. Canal, *ACS Appl. Mater. Interfaces* **2020**, *12*, 47256.
[24] X. Solé-Martí, T. Vilella, C. Labay, F. Tampieri, M.-P. Ginebra, C. Canal, *Biomater. Sci.* **2022**, *10*, 3845.
[25] H. Zhang, S. Xu, J. Zhang, Z. Wang, D. Liu, L. Guo, C. Cheng, Y. Cheng, D. Xu, M. G. Kong, M. Rong, P. K. Chu, *Biomaterials* **2021**, *276*, 121057.
[26] F. Abasalizadeh, S. V. Moghaddam, E. Alizadeh, E. Akbari, E. Kashani, S. M. B. Fazljou, M. Torbati, A. Akbarzadeh, *J. Biol. Eng.* **2020**, *14*, 8.
[27] M. I. Neves, L. Moroni, C. C. Barrias, *Front. Bioeng. Biotechnol.* **2020**, *8*, 665.
[28] A. Lin, J. De Backer, D. Quatannens, B. Cuypers, H. Verswyvel, E. C. De La Hoz, B. Ribbens, V. Siozopoulou, J. Van Audenaerde, E. Marcq, F. Lardon, K. Laukens, S. Vanlanduit, E. Smits, A. Bogaerts, *Bioeng. Transl. Med.* **2022**, *7*, e10314.
[29] D. S. Chen, I. Mellman, *Immunity* **2013**, *39*, 1.
[30] J. H. Lee, *Biomater. Res.* **2018**, *22*, 27.
[31] A. Espona-Noguera, J. Ciriza, A. Cañibano-Hernández, L. Fernandez, I. Ochoa, L. Saenz Del Burgo, J. L. Pedraz, *Int. J. Biol. Macromol.* **2018**, *107*, 1261.

[32] P. E. Ramos, P. Silva, M. M. Alario, L. M. Pastrana, J. A. Teixeira, M. A. Cerqueira, A. A. Vicente, *Food Hydrocolloids* **2018**, *77*, 8.
[33] P.-M. Girard, A. Arbabian, M. Fleury, G. Bauville, V. Puech, M. Dutreix, J. S. Sousa, *Sci. Rep.* **2016**, *6*, 29098.
[34] E. Freund, K. R. Liedtke, J. Van Der Linde, H.-R. Metelmann, C.-D. Heidecke, L.-I. Partecke, S. Bekeschus, *Sci. Rep.* **2019**, *9*, 634.
[35] W. Van Boxem, J. Van Der Paal, Y. Gorbanev, S. Vanuytsel, E. Smits, S. Dewilde, A. Bogaerts, *Sci. Rep.* **2017**, *7*, 106283.
[36] J. C. Mbongue, H. A. Nieves, T. W. Torrez, W. H. R. Langridge, *Front. Immunol.* **2017**, *8*, 327.
[37] A. Lin, M. Sahun, E. Biscop, H. Verswyvel, J. De Waele, J. De Backer, C. Theys, B. Cuypers, K. Laukens, W. V. Berghe, E. Smits, A. Bogaerts, *Drug Resist. Updat.* **2023**, *67*, 100914.
[38] X. Solé-Martí, C. Labay, Y. Raymond, J. Franch, R. Benitez, M.-P. Ginebra, C. Canal, *Plasma Processes Polym.* **2022**, *20*, 2200155.
[39] L. M. Nystrom, N. B. Reimer, J. D. Reith, M. T. Scarborough, C. P. Gibbs Jr., *Iowa Orthop J* **2016**, *36*, 98.
[40] J. Tornin, M. Mateu-Sanz, A. Rodríguez, C. Labay, R. Rodríguez, C. Canal, *Sci. Rep.* **2019**, *9*, 10681.